

The energy spectrum of all-particle cosmic rays around the knee region observed with the Tibet-III air-shower array

M.Amenomori^a, S.Ayabe^b, X.J.Bi^c, D.Chen^{d,*}, S.W.Cui^e,
Danzengluobu^f, L.K.Ding^c, X.H.Ding^f, C.F.Feng^g,
Zhaoyang.Feng^c, Z.Y.Feng^h, X.Y.Gaoⁱ, Q.X.Gengⁱ, H.W.Guo^f,
H.H.He^c, M.He^g, K.Hibino^j, N.Hotta^k, Haibing Hu^f, H.B.Hu^c,
J.Huang^l, Q.Huang^h, H.Y.Jia^h, F.Kajino^m, K.Kasaharaⁿ,
Y.Katayose^d, C.Kato^o, K.Kawata^l, Labaciren^f, G.M.Le^p,
A.F.Li^g, J.Y.Li^g, Y.-Q.Lou^q, H.Lu^c, S.L.Lu^c, X.R.Meng^f,
K.Mizutani^{b,r}, J.Muⁱ, K.Munakata^o, A.Nagai^s H.Nanjo^a,
M.Nishizawa^t, M.Ohnishi^l, I.Ohta^u, H.Onuma^b, T.Ouchi^j,
S.Ozawa^l, J.R.Ren^c, T.Saito^v, T.Y.Saito^l, M.Sakata^m,
T.K.Sako^l, T.Sasaki^j, M.Shibata^d, A.Shiomi^l, T.Shirai^j,
H.Sugimoto^w, M.Takita^l, Y.H.Tan^c, N.Tateyama^j, S.Torii^q,
H.Tsuchiya^x, S.Udo^l, B.Wangⁱ, H.Wang^c, X.Wang^l,
Y.G.Wang^g, H.R.Wu^c, L.Xue^g, Y.Yamamoto^m, C.T.Yan^l,
X.C.Yangⁱ, S.Yasue^y, Z.H.Ye^p, G.C.Yu^h, A.F.Yuan^f, T.Yuda^j,
H.M.Zhang^c, J.L.Zhang^c, N.J.Zhang^g, X.Y.Zhang^g, Y.Zhang^c,
Yi.Zhang^c, Zhaxisangzhu^f, X.X.Zhou^h,
(The Tibet AS γ Collaboration)

^a*Department of Physics, Hirosaki University, Hirosaki 036-8561, Japan*

^b*Department of Physics, Saitama University, Saitama 338-8570, Japan*

^c*Key Laboratory of Particle Astrophysics, Institute of High Energy Physics,
Chinese Academy of Sciences, Beijing 100049, China*

^d*Faculty of Engineering, Yokohama National University, Yokohama 240-8501,
Japan*

^e*Department of Physics, Hebei Normal University, Shijiazhuang 050016, China*

^f*Department of Mathematics and Physics, Tibet University, Lhasa 850000, China*

^g*Department of Physics, Shandong University, Jinan 250100, China*

^h*Institute of Modern Physics, South West Jiaotong University, Chengdu 610031,
China*

ⁱ*Department of Physics, Yunnan University, Kunming 650091, China*

^j*Faculty of Engineering, Kanagawa University, Yokohama 221-8686, Japan*

^k*Faculty of Education, Utsunomiya University, Utsunomiya 321-8505, Japan*

^ℓ*Institute for Cosmic Ray Research, University of Tokyo, Kashiwa 277-8582,
Japan*

^m*Department of Physics, Konan University, Kobe 658-8501, Japan*

ⁿ*Faculty of Systems Engineering, Shibaura Institute of Technology, Saitama
337-8570, Japan*

^o*Department of Physics, Shinshu University, Matsumoto 390-8621, Japan*

^p*Center of Space Science and Application Research, Chinese Academy of Sciences,
Beijing 100080, China*

^q*Physics Department and Tsinghua Center for Astrophysics, Tsinghua University,
Beijing 100084, China*

^r*Advanced Research Institute for Science and Engineering, Waseda University,
Tokyo 169-8555, Japan*

^s*Advanced Media Network Center, Utsunomiya University, Utsunomiya 321-8585,
Japan*

^t*National Institute of Informatics, Tokyo 101-8430, Japan*

^u*Tochigi Study Center, University of the Air, Utsunomiya 321-0943, Japan*

^v*Tokyo Metropolitan College of Industrial Technology, Tokyo 116-8523, Japan*

^w*Shonan Institute of Technology, Fujisawa 251-8511, Japan*

^x*RIKEN, Wako 351-0198, Japan*

^y*School of General Education, Shinshu University, Matsumoto 390-8621, Japan*

Abstract

We have already reported the first result on the all-particle spectrum around the knee region based on data from 2000 November to 2001 October observed by the Tibet-III air-shower array. In this paper, we present an updated result using data set collected in the period from 2000 November through 2004 October in a wide range over 3 decades between 10^{14} eV and 10^{17} eV, in which the position of the knee is clearly seen at around 4 PeV. The spectral index is $-2.68 \pm 0.02(\text{stat.})$ below 1 PeV, while it is $-3.12 \pm 0.01(\text{stat.})$ above 4 PeV in the case of QGSJET+HD model, and various systematic errors are under study now.

Key words: cosmic rays, knee, air shower

PACS: 98.70.Sa, 95.85.Ry, 96.40.De

* Corresponding author.

Email address: chen@icrr.u-tokyo.ac.jp (D.Chen).

1 Introduction

The energy spectrum of primary cosmic rays is well described by a power law over a wide energy range, while its slope becomes steeper in the energy range between 10^{15} and 10^{16} eV, which is called "knee". It has been discussed that the knee is closely related with the origin, the acceleration and the propagation of high-energy cosmic rays in the Galaxy. One of the plausible understanding may be that almost all cosmic rays below the knee are accelerated at supernova remnants (SNRs), since the maximum energy gained by shock acceleration at SNRs is of the order of 10^{14} eV per unit charge [Lagage and Cesarsky. 1983], the cosmic-ray spectrum is expected to become steeper at energies around and beyond the knee. Another possibility is that the break of the spectrum around the knee represents the energy at which cosmic rays can escape more freely from the trapping zone in the Galactic disk [Peters 1961].

We have already reported the first result on the all-particle spectrum around the knee region based on data from 2000 November to 2001 October observed by the Tibet-III air-shower array [Amenomori et al., 2003]. In this paper, we present an updated result using data set collected in the period from 2000 November through 2004 October. We also examine the simulation code CORSIKA with interaction models of QGSJET01c. Based on these calculations, we obtained the cosmic ray energy spectrum in a wide range over 3 decades between 10^{14} eV and 10^{17} eV.

2 Tibet-III air shower array and detector response

The Tibet-III air-shower array, consisting of 533 scintillation detectors of each 0.5 m^2 with the area of $22,050 \text{ m}^2$, has been successfully operating since 1999 with energy threshold of a few TeV. A 0.5 cm-thick lead plate is put on the top of each detector to increase the detection sensitivity of a detector by converting secondary gamma rays into electron-positron pairs in an air shower. In the fall of 2000, this array was further improved for UHE cosmic-ray study by adding wide dynamic range PMTs to all 221 sets of detectors which are placed on a lattice of 15 m spacing in the detector covering area of $36,900 \text{ m}^2$. This PMT equipped in each detector can measure the number of particles beyond 4,000, so that the array can observe UHE cosmic rays with the energy exceeding 10^{17} eV with a good accuracy.

The Tibet-III air-shower array is able to measure the shower size and the arrival direction of each air shower. The air shower direction can be estimated with an inaccuracy smaller than 0.2° at energies above 10^{14} eV. The shower size N_e for each event is estimated by fitting the lateral particle density distribution

with the modified NKG structure function (see section 3.2). The primary energy of each air shower event is then estimated from the air shower size. The relation between the shower size and the primary energy is calculated based on the MC simulation as discussed later. In general, the “shower size” means the number of electrons and positrons in each air shower event. It cannot be, however, directly obtained by usual shower array using scintillators since these electromagnetic components cannot be discriminated from other charged particles such as muons and hadrons.

In our experiment, the number of particles detected by each scintillation detector is defined as the PMT output (charge) divided by that of the single peak, which is determined by a probe calibration using cosmic rays. For this purpose, a small scintillator of $25\text{ cm} \times 25\text{ cm} \times 3.5\text{ cm}$ thick with a PMT (H1949) is put on the top of the each detector during the maintenance period. This is called probe detector and is used for making the trigger of the each Tibet-III detector. These events triggered by the probe detector was also examined by a MC simulation. In this simulation, the primary particles were sampled in the energy range above the geomagnetic cutoff energy at Yangba-jing, and all secondary particles which pass through the probe detector and the Tibet-III detector were selected for the analysis. Since the value of PMT output is proportional to the energy loss of the particles passing through the scintillator, the peak position of the energy loss distribution is defined as the “energy deposit by a singly charged particle”. This value corresponds to the observed single peak of the probe calibration. The peak energy was calculated as 6.11 MeV for the Tibet-III detector configuration. We confirmed that the shape of the energy loss distribution shows a good agreement with the charge distribution of the experimental data as shown in Fig. 1. It should be noted that the dependences of the energy loss on particle type and its energy are adequately taken into account in this calibration.

For air-shower MC calculation at high energies, we treat the number of shower particles as the calculated energy deposit divided by 6.11 MeV. Thus, all detector responses including muons and the materialization of photons inside the detector are taken into account. The shower size of each event was estimated using a modified NKG lateral distribution function which is tuned to reproduce the above defined lateral distribution using the MC events under our detector configurations.

3 Air shower size and primary particle energy

An extensive Monte Carlo simulation (MC) using CORSIKA code (ver. 6.204) including QGSJET01c [Heck et al., 1998] hadronic interaction model was made to obtain the primary cosmic ray spectrum using the Tibet-III air shower data.

Since the Tibet hybrid experiment of the air shower array and the burst detector array to measure the energy spectrum of the light components (proton and helium) strongly suggests that the knee region is dominated by heavy components [Amenomori et al., 2006], in this paper we use a heavy dominant (HD) composition model [Amenomori et al., 2000] in the MC for comparison with experimental data. All secondary particles are traced until their energies become 1 MeV in the atmosphere. Simulated air-shower events were input to the detector with the same detector configuration as the Tibet-III array with use of Epics code (ver. 8.64) [Kasahara] to calculate the energy deposit of these shower particles.

3.1 Event selection and collecting area

Following criteria are applied to select the events for the analysis.

- 1) The zenith angle (θ) of each air-shower event should be smaller than 25° , or $\sec \theta \leq 1.1$ to exclude the zenith angle dependence of the air-shower development.
- 2) More than 10 detectors should detect a signal of more than five particles per detector.
- 3) The central positions weighted by the 8th power of the number of particles at each detector should be inside the innermost $135 \text{ m} \times 135 \text{ m}$ area. This area is chosen with use of MC events so that the following two cases are just canceling out each other. Namely, the number of events originally inside of this area falling outside of this area after event reconstruction equals to the number of events in the opposite case.

It is confirmed by simulations that the air showers induced by primary particles with $E_0 \geq 100 \text{ TeV}$ and $\sec \theta \leq 1.1$ can be fully detected without any bias under above mentioned criteria.

The total effective area $S \times \Omega$ is calculated to be $10410.1 \text{ m}^2 \cdot \text{sr}$ for all primary particles with $E_0 \geq 100 \text{ TeV}$. For the operation period from 2000 November through 2004 October, the effective live time T is 2.21 years. The total number of air showers selected under the above conditions is 4.1×10^7 events.

3.2 Lateral distribution of shower particles

The determination of the lateral distribution function of an air shower is substantially important in this experiment, since the total number of shower par-

ticles is obtained by fitting the structure function to the experimental data. Since our air-shower array is also used to study the TeV gamma-ray point sources, lead plate of 5 mm thick is placed above each scintillation counter to increase the sensitivity, the detector response should be carefully examined by MC. Using the Monte Carlo data obtained under the same conditions as the experiment, we find that the following modified NKG function can fit well to the lateral distribution of shower particles under the lead plate:

$$f(r, s) = \frac{N_e}{C(s)} \left(\frac{r}{r_m'}\right)^{a(s)} \left(1 + \frac{r}{r_m'}\right)^{b(s)} / r_m'^2 \quad (1)$$

$$C(s) = 2\pi B(a(s) + 2, -b(s) - a(s) - 2) \quad (2)$$

where $r_m' = 30$ m, and the variable s corresponds to the age parameter, N_e the total number of shower particles and B denotes the beta function. The functions $a(s)$ and $b(s)$ are determined as follows. In CORSIKA simulation, the shower age parameter s is calculated at observation level by fitting to a function for the one dimensional shower development. It may be possible to assume that air showers with the same shower age s are in the almost same stage of air shower development in the atmosphere, i.e. they show the almost same lateral distribution for shower particles irrespective of their primary energies. The lateral distribution of the particle density obtained by the simulation with carpet array configuration is normalized by the total number of particles which is derived from the total energy deposit in infinitely wide scintillator. These events are then classified according to the stage of air shower development using the age parameter and they are averaged over the classified events. The fitting of the equation (1) to the averaged MC data is made to obtain the numerical values a and b . Thus, we can obtain the behavior of a and b as a function of s as shown in Fig. 2 where original definitions of $a(s)$ and $b(s)$ in NKG function are shown by the dotted lines. Although our result shows different dependences of a and b on s , it is confirmed that the lateral distribution of the shower particles is better reproduced by our formula. This expression is valid in the range of $s = 0.6 \sim 1.6$, $\sec \theta < 1.1$ and $r = 5 \sim 3000$ m.

Based on the Monte Carlo simulation, the correlation between the true shower size and the estimated shower size is demonstrated in Fig. 3(a) and Fig. 3(b). As seen in these two figures, a good correlation between the true shower size and the estimated shower size is obtained and the shower size resolution is estimated to be 7% above $N_e \geq 10^5$ with $\sec \theta \leq 1.1$.

3.3 Relation between the shower size and the primary energy

In Fig. 4, we show the correlation between the shower size N_e under the lead plate at the Tibet observation level and the primary energy E_0 for the QGSJET+HD model. The conversion function from the shower size N_e to the primary energy E_0 can be expressed by the following equation for $\sec \theta \leq 1.1$,

$$E_0 = a \times \left(\frac{N_e}{1000} \right)^b \quad [\text{TeV}], \quad (3)$$

where $a=1.88$, $b=0.92$. The energy resolution is estimated by our simulation as 36% and 17% at energies around 200 TeV and 2000 TeV, respectively. It is seen that the energy estimation of the primary particle from the air shower size is well made with a good accuracy in the wide energy range including the knee region. We further examine the dependence of the result on the interaction models, primary models, and other possible systematic biases in the very near future.

4 Results and Discussions

We obtained the all-particle energy spectrum between 1×10^{14} eV and 1×10^{17} eV based on the QGSJET+HD model as shown in Fig. 5. The red circle represents this work, and the blue inverse-triangle is our old result [Amenomori et al., 2003], and they are compared with other experiments. Our new result shows a good agreement with the previous one in the energy range less than 4 PeV, while suggesting a slightly steeper power index above 4 PeV and about 10% lower intensity around 10^{16} eV. This difference may be due to the upgrade of MC calculations and the increase of the observed data. The spectral index of this work is $-2.68 \pm 0.02(\text{stat.})$ below 1 PeV and $-3.12 \pm 0.01(\text{stat.})$ above 4 PeV in the case of QGSJET+HD model. The evaluation of various systematic errors is under examination at present.

The all-particle spectrum obtained in a wide range over 3 decades between 10^{14} eV and 10^{17} eV clearly shows the position of the knee being at energy around 4 PeV. In this work, we obtained the result based on the assumption that the knee energy region is dominated by nuclei heavier than helium [Amenomori et al., 2006]. It is noted that the all-particle spectrum depends slightly on the primary composition in the energy region below about 5×10^{14} eV. A further study of the dependence of the spectrum on the simulation codes, interaction models, primary composition models, and other possible systematic biases should be carefully done in the very near future.

Acknowledgments

The collaborative experiment of the Tibet Air Shower Arrays has been performed under the auspices of the Ministry of Science and Technology of China and the Ministry of Foreign Affairs of Japan. This work was supported in part by Grants-in-Aid for Scientific Research on Priority Areas (712) (MEXT), by Scientific Research (JSPS) in Japan, by the National Natural Science Foundation of China, and by the Chinese Academy of Sciences.

References

- [Amenomori et al., 1996] Amenomori, M., Cao, Z., Dai, B.Z., et al., The Cosmic-Ray Energy Spectrum between $10^{14.5}$ and $10^{16.3}$ eV Covering the “Knee” Region, *ApJ*. **461**, pp.408-414, 1996.
- [Amenomori et al., 2000] Amenomori, M., Ayabe, S., Caidong, et al., Measurement of air-shower cores to study the cosmic ray composition in the knee energy region, *Phys. Rev. D* **62**, pp.072007-1-12, 2000.
- [Amenomori et al., 2003] Amenomori, M., Ayabe, S., Cui, S.W., et al., The energy spectrum of all-particle cosmic rays around the knee region observed with the Tibet air-shower array, *Proc. 28th Int. Cosmic Ray Conf. (Tsukuba)*, Vol.1, pp.143-146, 2003.
- [Amenomori et al., 2006] Amenomori, M., Ayabe, S., Chen, D., et al., Are protons still dominant at the knee of the cosmic-ray energy spectrum?, *Phys. Lett. B* Vol.632, Issue 1, pp.58-64, 2006.
- [Antoni et al., 2005] Antoni, T., Apel, W.D., Badea, A.F., et al., KASCADE measurements of energy spectra for elemental groups of cosmic rays: Results and open problems, *Astropart. Phys.* **24**, pp.1-25, 2005.
- [Apanasenko et al., 2001] Apanasenko, A.V., Sukhadolskaya, V.A., Derbina, V.A., et al., Composition and energy spectra of cosmic-ray primaries in the energy range 10^{13} - 10^{15} eV/particle observed by Japanese-Russian joint balloon experiment, *Astropart. Phys.* **16**, pp.13-46, 2001.
- [Asakimori et al., 1998] Asakimori, K., Burnett, T.H., Cherry, M.L., et al., Cosmic-Ray Proton and Helium Spectra : Results from the JACEE Experiment, *ApJ* **502**, pp.278-283, 1998.
- [Glasmacher et al., 1999] Glasmacher, M.A.K., Catanese, M.A., Chantell, M.C., et al., The cosmic ray energy spectrum between 10^{14} and 10^{16} *Astropart. Phys.* **10**, pp.291-302, 1999.
- [Grigorov et al., 1971] Grigorov, N.L., Gubin, Yu.V., Jakovlev, B.M., et al., Energy Spectrum of Primary Cosmic Rays in the 10^{11} - 10^{15} eV According to the Data

of Proton-4 Measurements. Proc. 12th Int. Cosmic Ray Conf. (Hobart), Vol.5, pp.1746-1749, 1971.

[Heck et al., 1998]

Heck, D., et al., Report **FZKA 6019**, 1998 ; http://www-ik3.fzk.de/~heck/corsika/physics_description/corsika_phys.html.

[Kasahara] Kasahara,

K.,

<http://cosmos.n.kanagawa-u.ac.jp/EPICSHome/index.html>.

[Lagage and Cesarsky. 1983] Lagage, P.O. and Cesarsky, C.J., Cosmic-ray shock acceleration in the presence of self-excited waves, *Astron. Astrophys.* **118**, pp.223-228, 1983.

[Nagano et al., 1984] Nagano, M., Hara, T., Hatano, Y., et al., Energy spectrum of primary cosmic rays between $10^{14.5}$ - 10^{18} eV, *J. Phys. G* **10**, pp.1295-1310, 1984.

[Ogio et al., 2004] Ogio, S., Kakimoto, F., Kurashina, Y., et al., The energy spectrum and the chemical composition of primary cosmic rays with energies from 10^{14} to 10^{16} eV, *ApJ.* **612**, pp.268-275, 2004.

[Peters 1961] Peters, B., Primary Cosmic Radiation and Extensive Air Showers, *Nuovo Cimento* **22**, pp.800-806, 1961.

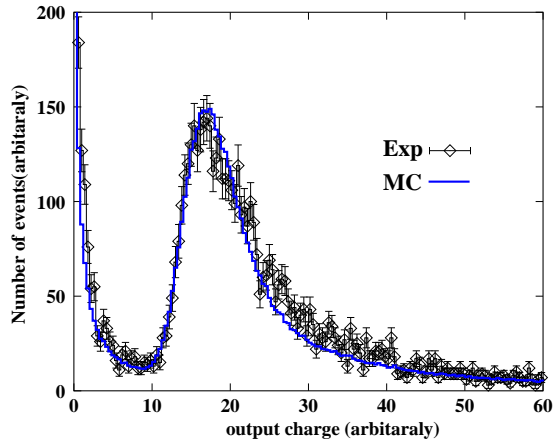


Fig. 1. Distribution of the output charge of PMT by probe calibration of the Tibet-III detector. In order to compare with the simulation on the energy deposit, the MC result is adjusted by multiplying a constant to meet with the same peak position as the experiment. The fluctuation of the number of photons in scintillation light is taken into account with the normal distribution in MC.

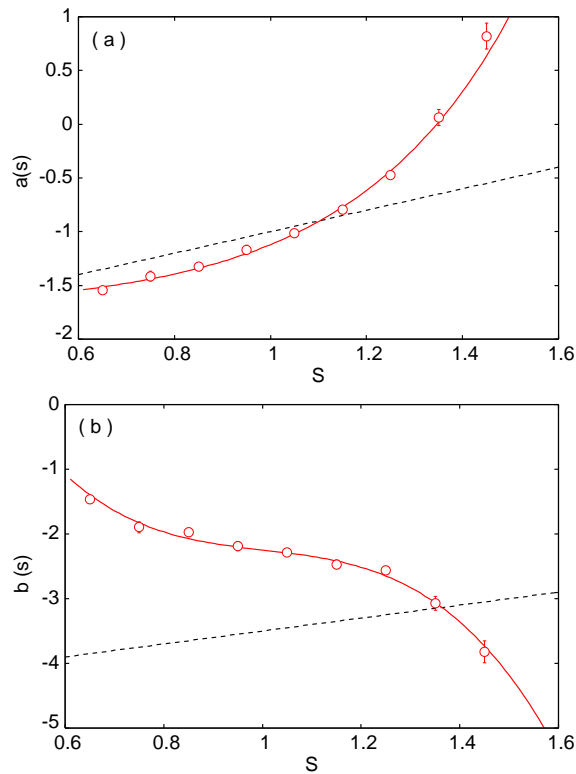


Fig. 2. The numerical values of a and b are plotted as a function of s , where original definitions of $a(s)$ and $b(s)$ in NKG function are shown by the dotted lines, and the open circles denote the averaged MC data which are fitted by empirical formulae shown by red lines. See the text.

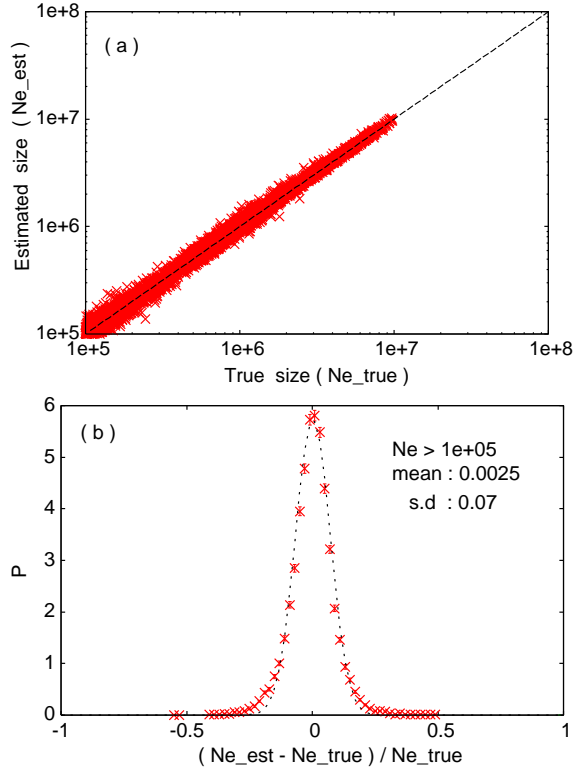


Fig. 3. (a) The correlation between the true shower size ($N_{e_{true}}$) and the estimated shower size ($N_{e_{est}}$). (b) The shower size resolution is estimated to be 7% above $N_e > 10^5$ with $\sec \theta \leq 1.1$.

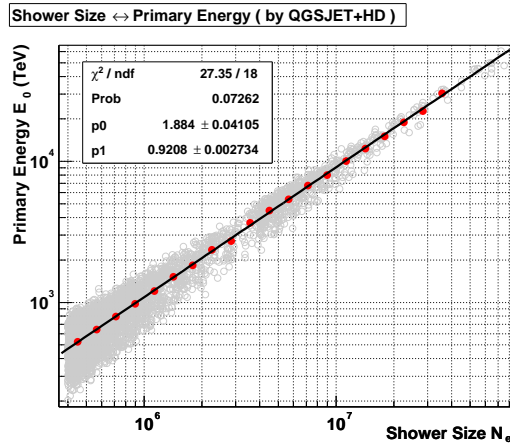


Fig. 4. Correlations of the air-shower size N_e and the primary energy E_0 at the Tibet observation level for the QGSJET+HD model with $\sec \theta \leq 1.1$. The solid circles denote the average values, and the solid lines is a fit by equation (3)

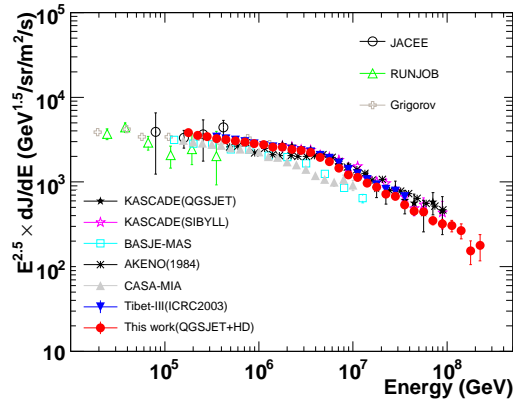


Fig. 5. Differential all-particle cosmic-ray flux in a wide range over 3 decades between 10^{14} eV and 10^{17} eV measured by the Tibet-III air-shower array using the QGSJET+HD model. This work is compared with other experiments : (JACEE [Asakimori et al., 1998], RUNJOB [Apanasenko et al., 2001], PROTON satellite [Grigorov et al., 1971], KASCADE [Antoni et al., 2005], BASJE-MAS [Ogio et al., 2004], AKENO [Nagano et al., 1984], CASA-MIA [Glasmacher et al., 1999], Tibet-III [Amenomori et al., 2003]).